Towards Biohybrid Lung Development? Inflammatory Conditions Disrupt Endothelial Layer Integrity on Gas Exchange Membranes

Maria Cheremkhina[1], Aaron Babendreyer[2], Christopher T. Neullens[3], Susanne Krapp[1], Alessa Pabst[2], Kim Ohl[3], Klaus Tenbrock[3], Stephan Ruetten[4], Andreas Ludwig[2], Christian G. Cornelissen[1,5], Anja Lena Thiebes[1]*, Stefan Jockenhoevel[1,6,]*

Affiliations:

[1] Department of Biohybrid & Medical Textiles (BioTex), Institute of Applied Medical Engineering, Helmholtz Institute Aachen, RWTH Aachen University, Forckenbeckstraße 55, 52074 Aachen, Germany

[2] Institute of Molecular Pharmacology, University Hospital RWTH Aachen, Wendlingweg 2, 52074 Aachen, Germany

[3] Division of Pediatric Immunology, Department of Pediatrics, RWTH Aachen University, Pauwelsstraße 30, 52074 Aachen, Germany

[4] Institute of Pathology, Electron Microscopy Facility, RWTH Aachen University Hospital, Aachen, Germany

[5] Department of Pneumology and Internal Intensive Care Medicine, Medical Clinic V, University Hospital RWTH Aachen, Pauwelsstraße 30, 52074 Aachen, Germany

[6] Aachen-Maastricht Institute for Biobased Materials, Faculty of Science and Engineering, Maastricht University, Brightlands Chemelot Campus, 6167 RD, Geleen, The Netherlands

Corresponding author: Anja Lena Thiebes (thiebes@ame.rwth-aachen.de)

*These authors have contributed equally

Abstract

Next to limited hemocompatibility, inflammation and sepsis are frequent complications during extracorporeal membrane oxygenation. Endothelialization of gas exchange membranes has been proposed to overcome these limitations and its general feasibility was demonstrated. However, these investigations focused on application of biohybrid devices under standard culture conditions neglecting patients' inflammatory status in future application. In this study, we investigate endothelial layer behavior on gas exchange membranes under inflammatory conditions in a microfluidic model system using immunocytochemistry, scanning electron microscopy, flow cytometry and qPCR. While co-culture with peripheral blood mononuclear cells (PBMCs) does not change endothelial layer integrity, confluence of endothelial cells is substantially reduced during inflammation via LPS-

activated PBMCs. Cell adhesion molecules were increasingly expressed under inflammatory conditions, consistent with an increased leukocyte adhesion. An upregulation of several genes linked to inflammation is observed: ICAM-1, VCAM-1, E-Selectin, IL6, IL8, IL10, and MCP-1. Our findings suggest that endothelial cells may struggle to maintain layer integrity within a biohybrid device when exposed to inflammatory conditions. This raises the question of whether endothelialization is an effective advancement of current technologies considering inflammation in patients. Yet the presented setup qualifies as sepsis in vitro model replicating the physiological vascular leak phenomenon to aid future investigations in biohybrid lung research.

Keywords

Dynamic culture, Sepsis, Human umbilical vein endothelial cells (HUVECs), Peripheral blood mononuclear cells (PBMCs), Lipopolysaccharides (LPS)

1. Introduction

Extracorporeal membrane oxygenation (ECMO) is an important treatment option for patients with severe respiratory failure, taking over their lung function for a short-term period [1, 2]. The only currently available long-term solution is lung transplantation. A major challenge restricting long-term use of ECMO systems is the insufficient hemocompatibility of the devices, characterized by high thrombo- and immunogenicity of oxygenator membranes [3-5].

To overcome these limitations, endothelialization of gas transfer membranes has been proposed by us and other groups [6-10]. Even though general feasibility of this concept has been demonstrated under standard cell culture conditions in vitro, these conditions do not reflect in vivo conditions during patient treatment [7, 11, 12]. Increased cytokine expression in the circulation is characteristic of most patients undergoing ECMO treatment, as respiratory failure is often accompanied by inflammatory conditions, such as pneumonia or sepsis during acute respiratory distress syndrome (ARDS) [13, 14]. ECMO is often used as a treatment for chronic obstructive pulmonary disease (COPD), which is characterized by inflammation [15, 16]. Additionally, it has been reported that ECMO treatment can induce systemic inflammatory response syndrome (SIRS), which leads to increased mortality [17, 18].

Endothelial cell behavior under inflammatory conditions has been extensively investigated [19-21]. While endothelial barrier function is maintained in healthy conditions by endothelial cell glycocalyx and intercellular junctions, increased cytokine production during inflammation causes upregulation of adhesion molecules, which in turn allows for leukocyte adhesion and transmigration [22-25]. The disruption of endothelial cell-cell junctions enables desired migration of leukocytes towards the inflamed tissue [26].

While immune cell activation and transendothelial cell migration are essential processes for tissue healing, disruption of intercellular junctions in an endothelialized oxygenator would lead to exposure of non-endothelialized gas exchange membrane to the blood. This could

consequently increase oxygenator membrane thrombogenicity and counteract the aim of the biohybrid lung concept.

In the current study, we investigated the behavior of endothelial cells on gas exchange membranes under inflammatory conditions. Dynamically cultured endothelial cells were treated with lipopolysaccharide (LPS)-activated peripheral blood mononuclear cells (PBMCs) to mimic inflammatory conditions. Endothelial cell layer integrity and expression of adhesion molecules were evaluated as well as leukocyte adhesion to the endothelial cells. Finally, changes in gene expression of endothelial cells under inflammatory conditions were investigated.

2. Materials and Methods

2.1. Isolation and Culture of Human Umbilical Vein Endothelial Cells

Human umbilical vein endothelial cells (HUVECs) were isolated from umbilical cords according to an established protocol [27]. Umbilical cords were obtained from the Clinic for Gynaecology and Obstetrics RWTH Aachen University Hospital after approval by the local ethics committee of the Medical Faculty of RWTH Aachen University Hospital (EK 067/18). All patients provided informed written consent. Briefly, HUVECs were dissociated with collagenase solution (1 mg/mL, Sigma-Aldrich) after washing the umbilical vein with Dulbecco´s Balanced Salt Solution (DPBS, Thermo Fisher Scientific). Culture of HUVECs was performed in endothelial cell growth medium 2 (EGM2, Promocell) with 1% antibiotic-antimycotic solution (ABM, Thermo Fischer) on gelatin-coated (2%, Sigma-Aldrich) tissue-culture flasks (Greiner) in a humidified incubator at 37 °C and 5% CO_2. Characterization of HUVECs was performed by flow cytometry analysis for CD31, CD105, CD144, CD146, and CD90. As shown in the supplementary Table S1, HUVECs were positive for CD31, CD105, CD144, and CD146, and negative for CD90, which confirmed their endothelial cell characteristics. HUVECs ($n = 3$ independent donors) were used in passage 4 for all experiments.

2.2. Isolation of Peripheral Blood Mononuclear Cells

Peripheral blood mononuclear cells (PBMCs) were isolated from freshly drawn venous blood. Blood was obtained from healthy male donors between 25 and 35 years of age after approval by the local ethics committee of the Medical Faculty of RWTH Aachen University Hospital (EK 22-390) and providing informed written consent. Blood was diluted with DBPS (mixing ratio 1:1) and mixed carefully. Blood/DPBS solution was slowly pipetted onto Pancoll (Pan-Biotech) (ratio of Pancoll to blood/DPBS 1:2) to create a distinct separation line between Pancoll and blood/DPBS. After centrifugation for 30 min at 500 g at room temperature without brake, PBMCs were separated from granulocytes and erythrocytes and were identifiable as a cloudy dark-yellow layer on top of Pancoll. PBMCs were carefully transferred from the tubes and washed with DPBS. Erythrocyte lysis was performed according to manufacturer´s instructions by suspending PBMCs in erythrocyte lysis buffer (Pan-Biotech), followed by incubation for 5 min at room temperature. Lysis was stopped by the addition of EGM2. PBMCs were washed once again with DPBS before proceeding with further experiments. PBMCs were used directly after isolation for all experiments.

2.3. Static Culture of Endothelial Cells on Gas Exchange Membranes and Thrombin Generation Assay

Polydimethylsiloxane (PDMS) membranes (800 µm, Limitless Shielding) were washed with soap, absolute ethanol (70%, Merck), and ultra-pure water (Sartorius). Circular samples (6 mm diameter) were glued (Elastosil® E50 N Transparent silicon rubber, Wacker Chemie AG) to the bottom of 24-well plates (Greiner) and cured for at least 24 h at room temperature. PDMS membranes were functionalized with RGD peptides as previously described [28]. RGD is an amino acid sequence of arginine, glycine, and aspartic acid, and is a binding motif for cellular integrins. RGD functionalization allows cell attachment on otherwise highly hydrophobic PDMS membrane. Briefly, Sulfo-SANPAH (1 mmol/L, Thermo Fischer) was pipetted onto PDMS membranes, followed by exposure to UV light for 2 h. PDMS membranes were treated with GRGDS solution (1 mmol/L, Bachem AG) for 24 h after washing the membranes with DPBS. RDG-coated PDMS membranes (RGD-PDMS) were washed with DPBS and stored in DPBS at 4 °C for a maximum of 7 days before usage. HUVECs were resuspended in EGM2 containing 1% ABM and transferred to each well at a concentration of 7×10^5 cells/cm^2. Endothelial cells were incubated in a humidified incubator at 37 °C and 5% CO_2 for 24 h to allow cell attachment. The membranes were checked for full confluence before performing the thrombin generation assay.

To evaluate the thrombogenicity of the biofunctionalized and endothelialized membranes, a thrombin generation assay (TGA, Haemoscan) was performed. The membranes were carefully washed with DPBS, and the assay was performed according to the manufacturer's instructions compliant with ISO 10993-4:2017. Briefly, all samples were incubated with human plasma before adding the TGA reagents. Thrombin generation was measured at 1, 2, 3, and 4 min after reagent addition. Thrombin-specific chromogenic substrate was added, which results in a yellow-coloured product proportional to the amount of produced thrombin. The optical density was measured at 405 nm and 540 nm with a microplate reader (Infinite® 200Pro, Tecan). Thrombin concentration was calculated from calibration curves. The calculation of maximum thrombin generation was performed according to the manufacturer´s instructions. Briefly, the thrombin generation between the last two measured time points (3 and 4 min) was normalized to the membrane surface area, as the highest increase in generated thrombin occurred at that time.

2.4. Dynamic Culture of Endothelial Cells on Gas Exchange Membranes

PDMS membranes were washed as described above, followed by gluing of the membranes to the microfluidic devices (sticky Slides 0.2 Luer, Ibidi) with 250 µm channel height. The mounted devices were incubated in an oven for 8 h at 60 °C and then cooled to room temperature for full membrane attachment. RGD coating of PDMS membranes was performed as described above. For endothelialization, HUVECs were resuspended in EGM2 medium with 1% ABM at a concentration of 5×10^6 cells/mL and seeded in the microfluidic channels at a final cell concentration of 1.2×10^5 cells/cm^2. Microfluidic devices with seeded cells were incubated statically for at least 2.5 h until full cell attachment while medium exchange was carefully performed every 30 minutes. Afterwards, three microfluidic devices were connected in series to the bioreactor system. The bioreactor system was assembled using a syringe pump (LA-120, Landgraf Laborsysteme GmbH), syringe (B.Braun), gas filter (Merck), three-way valves

(B.Braun), one-way valves (CODAN Medizinische Geräte GmbH) and Heidelberger extensions (B.Braun) as shown in Figure 1. The inclusion of one-way valves allowed for one-directional flow inside the microfluidic chambers both during pushing and pulling phase of the syringe. The bioreactor system was assembled and cultured with EGM2 medium with 1% ABM at 37 °C and 5% CO_2 24 h prior to connection of microfluidic devices for system equilibration to reduce the amount of air bubbles in the tubing.

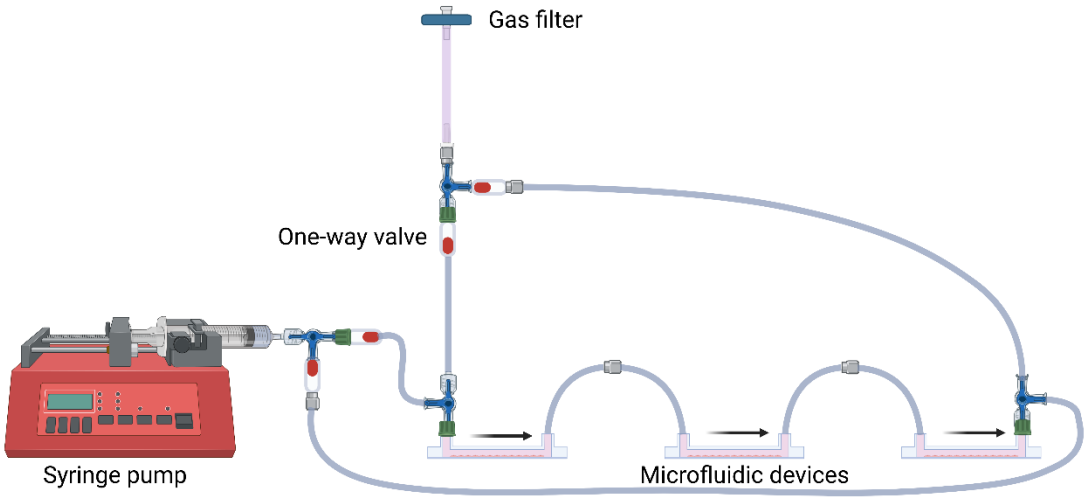

Figure 1. Bioreactor system with syringe pump and connected microfluidic devices. The flow direction in the microfluidic devices was kept constant during the experiment (indicated by the arrows) and the culture was performed in a controlled atmosphere (37 °C, 5% CO_2).

Laminar flow of 8.4 mL/min was applied to the cells in microfluidic devices, resulting in a wall shear stress (WSS) of 20 dyn/cm^2. After 24 h of endothelial cell dynamic culture under standard conditions, the experiment was performed with four different groups: 1) EGM2 served as control, 2) LPS was added to EGM-2 in a concentration of 100 ng/mL, 3) PBMCs were diluted in EGM2 with a final concentration of 1.5 × 10^6 cells/mL, 4) For imitation of inflammatory conditions, LPS-activated PBMCs were added to the culture system at the same concentrations. After 24 h culture under experimental conditions, the culture was terminated by either fixation of the cells with ice-cold methanol (VWR) for immunocytochemistry (ICC) and scanning electron microscopy (SEM), cell detachment with accutase (Innovative Cell Technologies) for flow cytometry, or cell lysis and RNA isolation for quantitative polymerase chain reaction (qPCR) analysis.

2.5. Leukocyte Adhesion Assay

For the leukocyte adhesion assay, PBMCs were stained with 5-chloromethylfluorescein diacetate (CMFDA, Thermo Fisher) prior to dynamic culture. PBMCs were incubated with Dulbecco's Modified Eagle's Medium (DMEM, Thermo Fisher) containing 1 µM CMFDA dye for 30 minutes at 37 °C. After washing the cells with EGM2, PBMCs were used for dynamic culture as described in Chapter 0. After dynamic culture, microfluidic devices with HUVECs and attached PBMCs were fixed with ice-cold methanol for 10 min at -20 °C, and carefully washed three times with DPBS. Microscopy of the endothelial cells with attached PBMCs was performed within one week after fixation (AxioObserver Z1, Carl Zeiss with AxioCam MRm with ZEN blue 3.6 software). Endothelialized area of each brightfield image was determined

with GNU Image Manipulation Program software (GIMP V2.10.34, The GIMP team), and the number of attached PBMCs was calculated with open-source CellProfiler software V4.2.5 [29].

2.6. Immunocytochemical Staining

After dynamic culture, HUVECs were fixed with ice-cold methanol for 10 min at -20 °C and washed three times with DPBS. The membranes were carefully cut out of the microfluidic devices, and ICC was performed with antibodies against CD31 and von Willebrand factor (vWf) as previously described [30]. Briefly, blocking with 3% bovine serum albumin (BSA, Sigma Aldrich) in DPBS was performed to block the non-specific binding sites. Following, the samples were incubated sequentially with primary antibodies against CD31 (1:100 in 3% BSA solution in DPBS, P8590 Sigma Aldrich) and vWf (1:100 in 0.1% Triton-X solution (Sigma Aldrich) in DPBS, A0082 Dako), and their respective secondary antibodies Alexa Fluor 594 goat anti-mouse (1:400 in 3% BSA solution in DPBS, A11005 Thermo Fischer Scientific) and Alexa Fluor 488 goat anti-rabbit (1:400 in 0.1% Triton-X solution in DPBS, A11008 Thermo Fischer Scientific) for 1 h each at 37 °C. DAPI (Carl Roth) was used to counterstain cell nuclei. For microscopy, a drop of mounting medium (Ibidi) was placed in a microscopy-suited µ-Slide chambered coverslip (Ibidi), and the PDMS membrane was placed into the chamber with the cell-side down. Microscopy was performed with an inverted confocal laser scanning microscope (LSM 980 with Airyscan 2, Zeiss).

2.7. Flow Cytometry Analysis

After dynamic culture, the cells were washed with DPBS, and treated with accutase for 3 minutes at 37 °C to ensure gentle cell detachment. After cell collection, live-dead staining (Zombie Aqua, BioLegend) of the cells was performed according to manufacturer's instructions. Briefly, cell suspension was incubated with the live-dead staining solution (1:1000 in DPBS with 1% fetal bovine serum (FBS, Capricorn)) for 30 minutes in the dark at room temperature. After washing the cells with DBPS, flow cytometry antibody staining was performed according to the manufacturer's instructions. The cell suspension was incubated with the following antibodies for 30 minutes at 4 °C: CD106-PE (VCAM-1, 555647, BD Biosciences), CD62E-FITC (E-Selectin, BBA21, R&D Systems), CD54 (ICAM-1, 555510, BD Biosciences). After washing the cell suspension, samples were incubated with the secondary antibody V450 (562107, BD Biosciences) for the CD54-primary antibody for 30 minutes at 4 °C. The cells were resuspended in DPBS with 1% FBS, and all measurements were performed with FACS Canto cytometer (BD Biosciences). Mean fluorescence intensities (MFI) of the adhesion molecule expression was evaluated and all data were processed using FlowJo software (V10.8.1, FlowJo LLC).

2.8. Scanning Electron Microscopy

SEM analysis was performed by the facility for electron microscopy of the medical faculty of RWTH Aachen University. The methanol-fixed samples were transferred to 3% glutaraldehyde solution (Agar scientific) in 0.1 M sodium phosphate buffer (Merck). Dehydration was performed with ascending ethanol series (30%; 50%; 70%; 90%; 100%; 100%; 100%). Critical point drying in liquid CO_2 (Polaron, Quorum Technologies Ltd) was performed before coating of the samples with a 10 nm gold/palladium layer (Sputter Coater EM SCD500, Leica). Scanning

electron microscopy was performed in a high vacuum environment at 10 kV voltage (Quattro S, Thermo Fischer Scientific).

2.9. Quantitative PCR Analysis

RNA was extracted from the cells after dynamic culture by removing the medium from the channels and adding the RLT buffer (RNeasy Kit, Qiagen) for cell lysis and consequent RNA isolation. For RNA isolation from PBMCs, medium suspension from dynamic culture was centrifuged at 500 g for five minutes and the pellet containing PBMCs was lysed with the RLT buffer before RNA isolation according to the manufacturer's protocol. Briefly, the lysed cell solution was loaded onto a separation column, followed by several washing steps. Finally, RNA was eluted with RNAse-free water. RNA was reverse transcribed using a PrimeScript™ RT Reagent Kit (Takara Bio Europe), and PCR reactions were performed using iTaq Universal SYBR Green Supermix (Bio-Rad), according to the manufacturers' protocols. The mRNA expression levels of VCAM-1, ICAM-1, E-selectin, IL-8, IL-6, IL-10, TNFα, MCP-1, TM, TPA, vWF, VE-cadherin, CD31, NOS3, EDN1 were measured using quantitative real-time PCR and normalized to the mRNA expression level of different reference genes. Supplemental table S3 describes all used primers and annealing temperatures. CFX Maestro Software 1.1 (Bio-Rad) was used to determine the most stable reference genes: eukaryotic translation initiation factor 4A2 (EIF4A2) and ribosomal protein L13A (RPL13A). The term reference gene index (ref. gene index) was introduced as the normalization was always performed against these two genes. All PCR reactions were run on a CFX Connect Real-Time PCR Detection System (Bio-Rad) using the following protocol: 40 cycles of 10 s denaturation at 95 °C followed by 10 s annealing and 15 s amplification at 72 °C. The uncorrected RFU values using LinRegPCR version 2020.0 were used to determine the PCR efficiency [31]. The CFX Maestro Software 1.1 (Bio-Rad) was used for the relative quantification, and the evaluation algorithm was based on the ddCt method.

Principal component analysis (PCA) was performed based on the qPCR data in Python using the Scikit-learn module [32]. The standardization of the data was performed using the StandardScaler of Scikit-learn prior to PCA. Plotly Express (Plotly Technologies Inc.) was used for the graphical representation of the results. The samples were coloured depending on the culture conditions. The loadings of the genes were plotted as arrows with the length of the arrow representing the value of the loadings.

2.10. Statistical Analysis

All experiments were performed with three biological replicates ($n = 3$). The results are presented in mean ± standard deviation. The data analysis was performed with Excel 2016 (Microsoft), and Prism 9 (9.4.0, Graphpad Software). Statistical evaluation of TGA and leukocyte adhesion assay was performed with Welch´s *t*-test and Mann-Whitney test, respectively. Flow cytometry and qPCR data were analyzed for the normal distribution using residual plots, Shapiro-Wilk and Kolmogorov-Smirnov tests as diagnostics. In case of normal distribution, ordinary one-way ANOVA with Tukey´s multiple comparisons test was performed for the statistical analysis. A non-parametric Kruskal-Wallis test was performed if no normal distribution was confirmed (Shapiro-Wilk and Kolmogorov-Smirnov tests). A p-value below 0.05 was considered statistically significant (labeled with *).

3. Results

3.1. Thrombin Generation on Endothelialized Gas Exchange Membranes

To investigate if endothelial cells improve hemocompatibility of our biofunctionalized PDMS gas exchange membranes, thrombin generation assay was performed according to ISO 10993-4:2017.

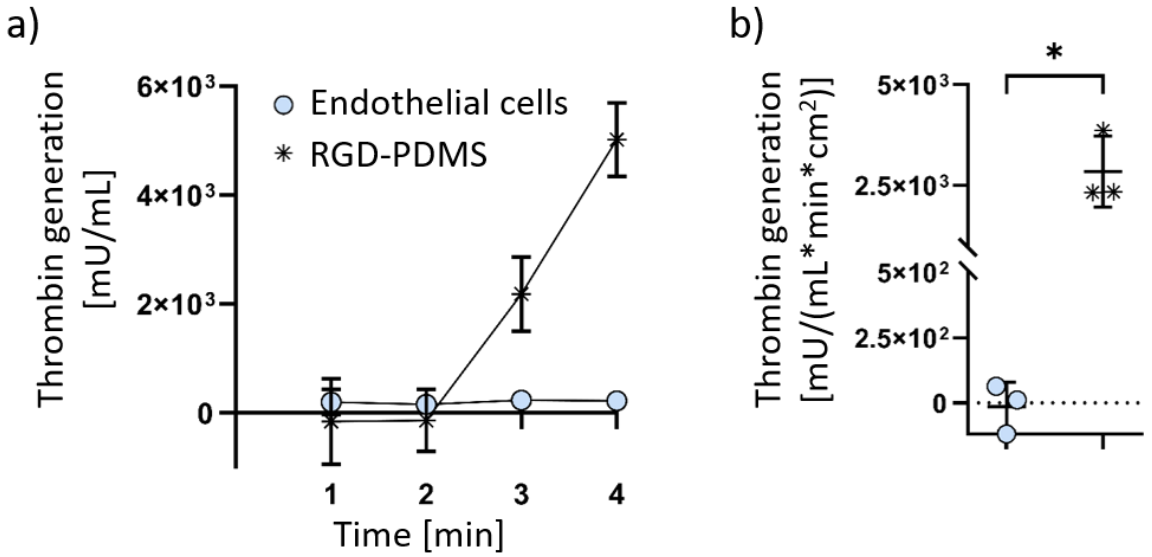

Figure 2. Thrombin generation on endothelialized PDMS membranes in comparison with non-endothelialized PDMS membranes. Thrombin generation over 4 minutes (a), and maximum thrombin generation during the assay (b) are shown. The data is shown as mean ± SD, with symbols in b) representing the individual data points. P-value below 0.05 was considered statistically significant (labelled with *).

Thrombin generation is significantly reduced for endothelialized PDMS membranes compared to cell-free membranes (Figure 2), with the maximum thrombin generation of RGD-PDMS membrane reaching $2.8 \times 10^3 \pm 8.8 \times 10^2$ mU/(mL x min x cm^2), whereas the confluent endothelial cell layer on the PDMS membrane shows no relevant thrombin generation (Figure 2b). Thrombin generation measurement over four minutes shows an increase in thrombin generation on RGD-PDMS in contrast to endothelialized membranes, on which no thrombin generation occurs during the measurement time (Figure 2a).

3.2. Morphology of Endothelial Cells during Dynamic Culture in Inflammatory Conditions

Maintenance of a confluent endothelial cell layer is essential for successful oxygenator membrane endothelialization. ICC staining and SEM were performed to evaluate the ability of endothelial cells to withstand WSS and preserve cell layer confluence during dynamic culture under inflammatory conditions (Figure 3d, Figure ***3***h). Endothelial cells dynamically cultured with either only LPS or PBMCs or in normal cell culture medium were used as controls (Figure 3a-c, Figure ***3***e-g).

Cell-cell adhesions are shown by CD31 staining (yellow), while vWF is found in the cytoplasm (pink). Culture of endothelial cells with either LPS or PBMCs does not change their morphology or expression pattern of CD31 (Figure 3e-g, a-c, respectively). In contrast, a loss of cell confluence is observed upon culture of endothelial cells under inflammatory conditions. The endothelial cell layer appears disrupted (Figure 3d, Figure 3h) and a substantial reduction of

CD31-cell-cell adhesions is confirmed by antibody staining (Figure 3d). vWF expression does not seem to be altered by culture under inflammatory conditions (Figure 3d) in comparison to the controls (Figure 3a-c).

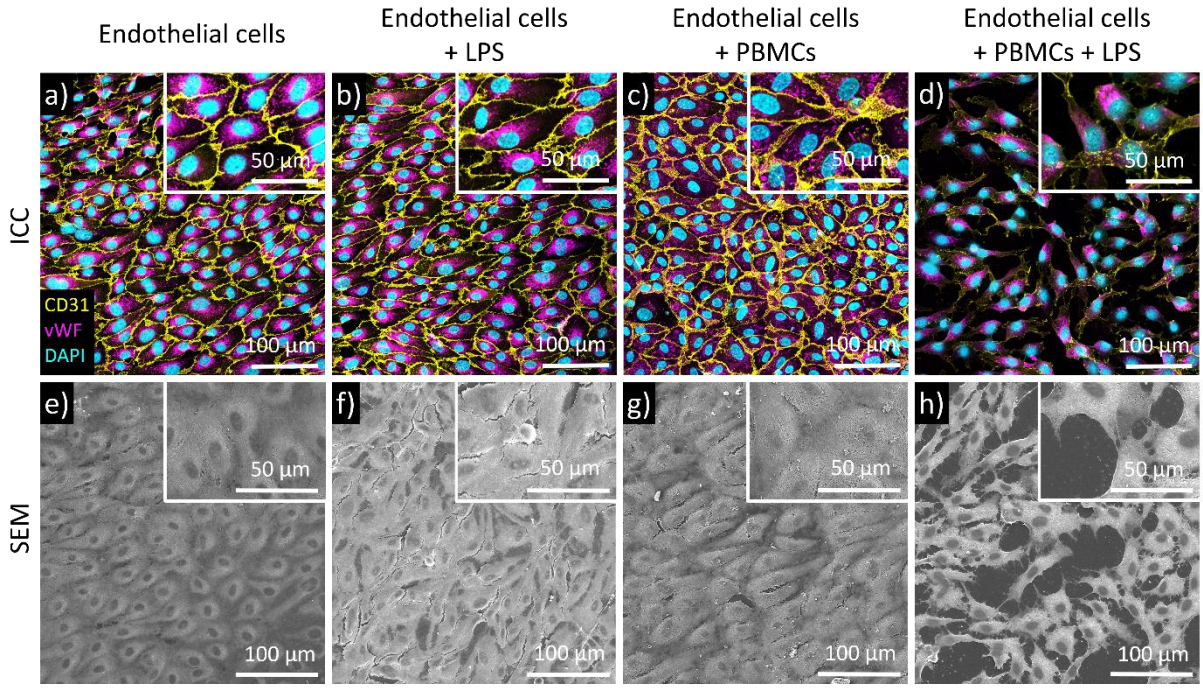

Figure 3. Evaluation of endothelial cell morphology. Immunocytochemical staining of endothelial cells against CD31 (yellow), vWF (purple), and DAPI (blue)-stained cell nuclei (a - d); scanning electron microscopy of endothelial cell layer after dynamic culture (e-h). Representative images of following conditions are shown: endothelial cells (medium control) (a, e); endothelial cells with LPS-treatment (b, f); endothelial cells cultured with PBMCs (c, g); endothelial cells cultured with LPS-treated PBMCs (d, h).

3.3. Leukocyte Adhesion on Endothelial Cells

Leukocyte adhesion to the endothelial cell layer is a key characteristic of inflammatory processes in vivo. In this work, it was directly and indirectly evaluated by performing a leukocyte adhesion assay (Figure 4a) and flow cytometry measurement of endothelial cell adhesion molecules ICAM-1, E-Selectin, and VCAM-1 (Figure 4b-g), respectively.

Adhesion of PBMCs is increased on endothelial cells under LPS-treatment (Figure 4a). In detail, 110 ± 31 PBMCs/mm adhere to endothelial cells during LPS-free culture, and 297 ± 107 PBMCs/mm to endothelial cells with LPS-treatment. Representative pictures of endothelial cells treated with stained PBMCs, with and without LPS activation, are shown in the supplementary Figure S1. Flow cytometry measurement reveals a significant increase in ICAM-1, E-Selectin, and VCAM-1 expression under culture of endothelial cells with LPS-activated PBMCs in comparison to the medium control (Figure 4b-g). A slight increase in ICAM-1, E-Selectin, and VCAM-1 expression is observed in endothelial cells cultured with LPS or PBMCs in comparison to non-treated cells, while all values are in the same order of magnitude. All MFI data of ICAM-1, E-Selectin, and VCAM-1 expression are shown in supplementary table S2.

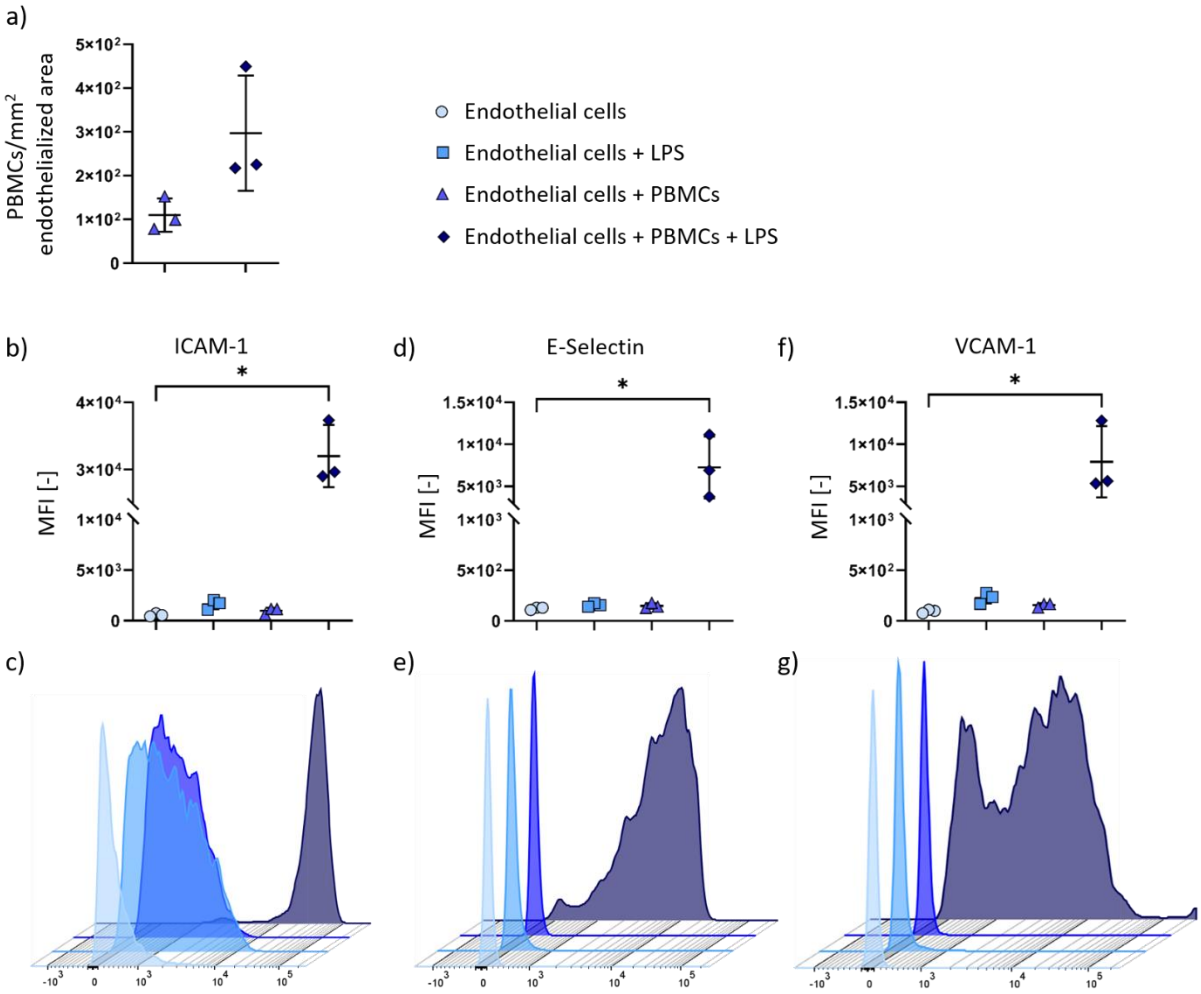

Figure 4. Leukocyte adhesion on endothelial cells (*n=3*) during dynamic culture under inflammatory conditions. Leukocyte adhesion assay (a) comparing PBMC-adhesion to endothelial cells with and without LPS-activation (*n=3*). Flow cytometry (b-g) of endothelial cells for following cell adhesion molecules: b), c): Intercellular adhesion molecule-1 (ICAM-1); d), e): E-Selectin; f), g): Vascular cell adhesion molecule 1 (VCAM-1). Mean fluorescent intensities (MFI) of adhesion molecules expression calculated from *n=3* independent donors are shown (b, d, f), as well as representative histograms (c, e, g). P-value below 0.05 was considered statistically significant (labelled with *).

3.4. Quantitative mRNA Analysis of Endothelial Cells Dynamically Cultured under Inflammatory Conditions

Endothelial cell behavior during dynamic culture under inflammatory conditions was evaluated by quantitative mRNA analysis. The results are shown in Figure 5.

Expression of the following genes was analyzed in the current study to investigate the inflammatory processes: ICAM-1, E-Selectin, VCAM-1, IL6, IL8 (gene CXCL8), IL10, TNFα, and MCP-1 (gene CCL2) (Figure 5a-h). The mRNA expression of endothelial adhesion molecules ICAM-1, VCAM-1, and E-Selectin was increased upon culture under inflammatory conditions (endothelial cells + PBMCs + LPS), with a significant result for ICAM-1 expression in comparison to the control. A higher expression of the pro-inflammatory genes IL6 and IL8, as well as the anti-inflammatory gene IL10 was similarly observed in endothelial cells cultured under inflammatory conditions, along with a significant increase in TNFα and MPC-1 expression. Interestingly, no significant differences are observed in the expression of the following genes involved in thrombogenicity regulation in endothelial cells: vWF, TM (gene

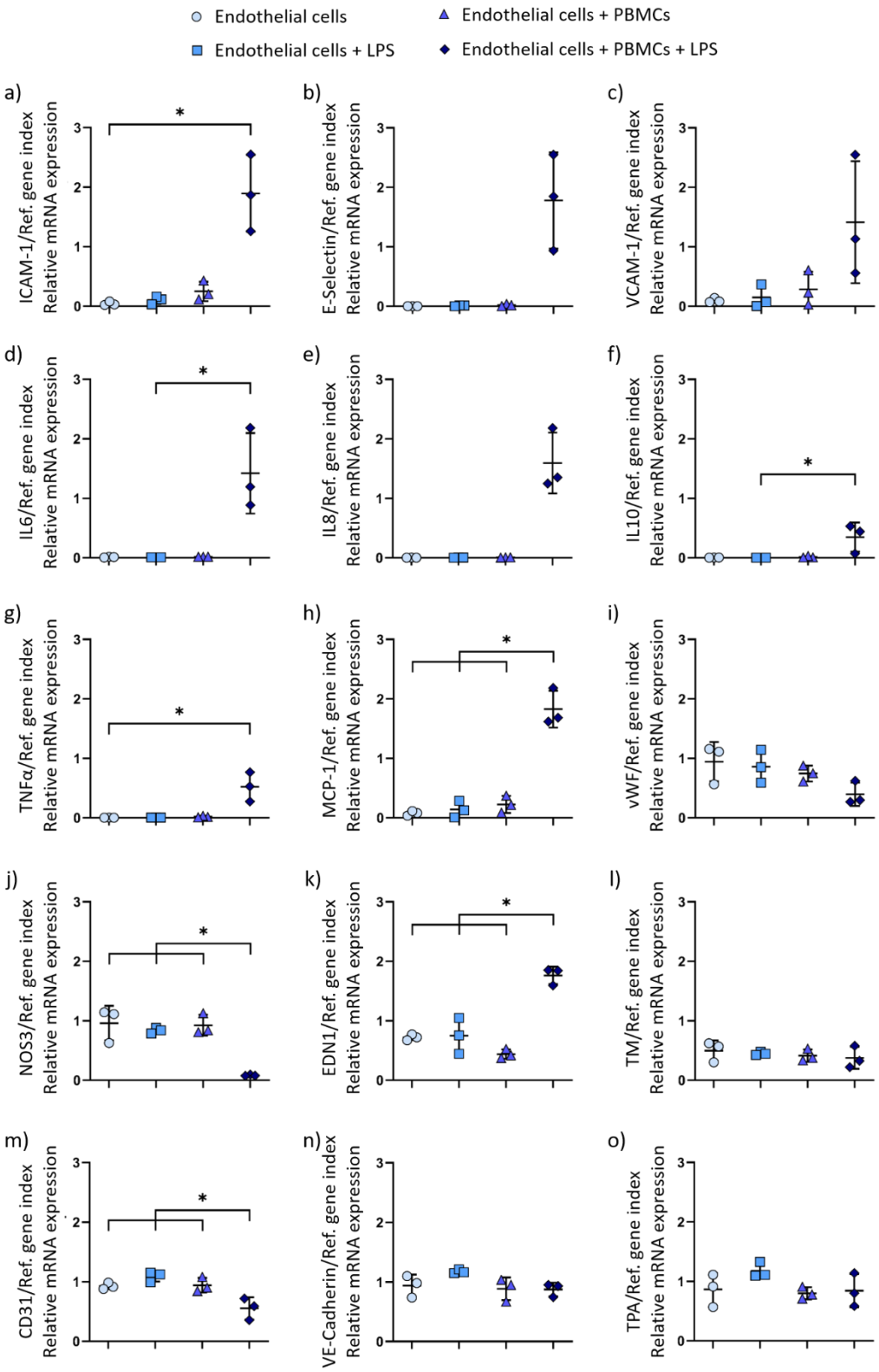

Figure 5. Relative mRNA expression in endothelial cells (*n=3*) after dynamic culture under inflammatory conditions (endothelial cells + PBMCs + LPS), with following groups as controls: endothelial cells, endothelial cells + LPS, endothelial cells + PBMCs. Endothelial cells were analysed for relative mRNA expression of a) Intercellular adhesion molecule-1 (ICAM-1); b) E-Selectin; c) Vascular cell adhesion molecule 1 (VCAM-1); d) Interleukin 6 (IL6); e) Interleukin 8 (IL8); f) Interleukin 10 (IL10); g) Tumor necrosis factor alpha (TNFα); h) Monocyte chemoattractant protein-1 (MCP-1); i) Von Willebrand factor (vWF); j) Nitric oxide synthase 3 (NOS3); k) Endothelin 1 (EDN1); l) Thrombomodulin (TM); m) Platelet and endothelial cell adhesion molecule 1 (PECAM-1, CD31); n) Vascular endothelial cadherin (VE-Cadherin); o) Tissue plasminogen activator (TPA) in relation to a reference gene index consisting of EIF4A2 and RPL13A. Data are shown as mean ± SD with symbols representing the individual data points. P-value below 0.05 was considered statistically significant (labelled with *).

THBD), and TPA (gene PLAT) (Figure 5i, Figure ***5***l, Figure ***5***o). NOS3 gene expression, which is responsible for the production of nitric oxide (NO), is significantly reduced, while its antagonist, EDN1, shows a significant increase in endothelial cells cultured under inflammatory conditions (Figure 5j-k). No change in VE-Cadherin (gene CDH5) expression is observed between all investigated conditions (Figure 5m). Expression of CD31 (gene PECAM-1), is significantly decreased in endothelial cells under inflammatory conditions (Figure 5n).

A multidimensional PCA was performed to further evaluate qPCR data (Figure 6). PCA showed a clear separation of endothelial cells dynamically cultured under inflammatory conditions (endothelial cells + PBMCs + LPS) from all other endothelial cell samples (endothelial cells, endothelial cells + PBMCs, and endothelial cells + LPS) (Figure 6a). Furthermore, full separation of PBMCs from all endothelial cell samples was observed, with an additional separation between the samples PBMCs and PBMCs + LPS (Figure 6a). Three big gene groups can be identified considering the loadings of the genes (Figure 6b). While the mRNA expression of ICAM-1, VCAM-1, E-Selectin, IL6, IL8, MCP-1, and EDN1 affect the positioning of endothelial cells cultured under inflammatory conditions, mRNA expression of VE-Cadherin, CD31, vWF, and NOS3 genes appears to be important for endothelial cells cultured under all other conditions (endothelial cells, endothelial cells + PBMCs, and endothelial cells + LPS). Dynamically cultured PBMCs (with and without LPS) strongly express TNFα and IL10 mRNA (Figure 6b).

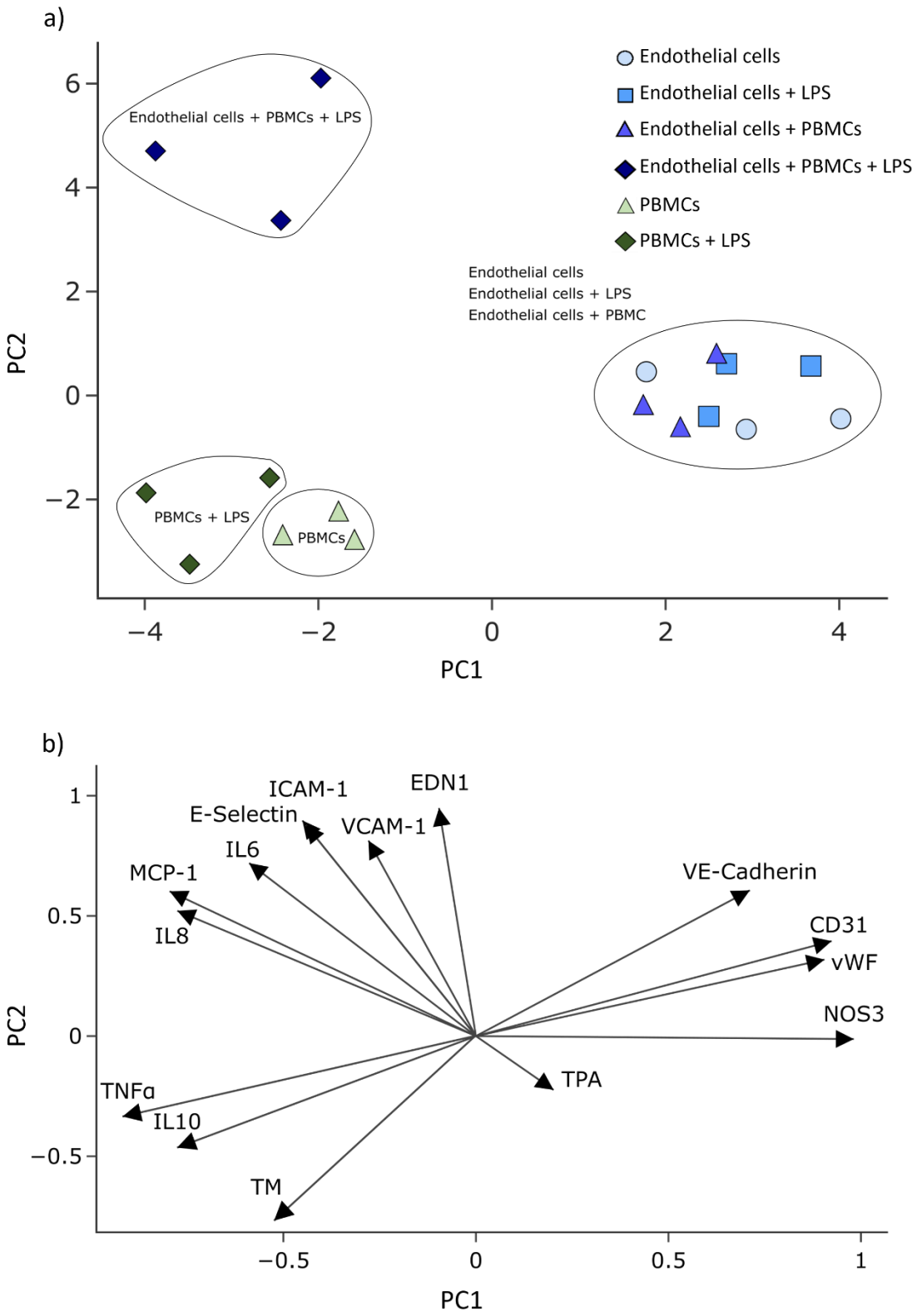

Figure 6. Principal component analysis of mRNA expression data. Results are presented as scattered plots where each symbol represents one sample. Samples are colored for the different culture conditions (a). The loadings of investigated genes are plotted as arrows (b).

4. Discussion

In the current study, we demonstrate the importance of mimicking physiological conditions closely *in vitro* for investigation of biohybrid devices. Endothelialization of gas exchange membranes has previously been investigated in several studies as a possible solution to overcome hemocompatibility issues of ECMO devices, with the main focus of research being proof-of-concept, as well as endothelialization techniques and the ability of endothelial cells to withstand long-term culture under increased wall shear stress (WSS) under 'healthy' conditions [7, 11, 12, 33, 34].

Here, we performed an ISO 10993-4:2002-compliant thrombin generation assay to quantify if the thrombogenicity of gas exchange membranes improves after endothelialization. Indeed, thrombin generation of endothelialized membrane is significantly lower than the bare membrane. This supports the general hypothesis that endothelialization of oxygenator membranes reduces membrane thrombogenicity and thus improves the devices' hemocompatibility. As the material thrombogenicity relies on its surface constitution, we assume that the thrombogenicity of endothelialized membrane would remain significantly lower than that of uncoated gas exchange membranes, as long as the endothelial cell layer is fully confluent and does not expose the membrane surface underneath it [35].

Apart from the high thrombogenicity of ECMO devices, an increased inflammatory response has been reported in most patients undergoing ECMO treatment [18]. Systemic inflammatory response is characterized by highly elevated pro- and anti-inflammatory cytokine levels [4]. It has been previously described that endothelial cells respond to inflammation with endothelial activation which might result in increased leukocyte adhesion, decreased barrier function, vasoconstriction, and vascular leakage and changes in thromboresistance [22]. This inflammation-induced vascular dysfunction is reversible with appropriate treatment [36]. To the authors' knowledge, no investigation of endothelial cell layer behavior on gas exchange membranes has been previously performed under inflammatory conditions. Thus, we developed a dynamic microfluidic culture system that allows for dynamic culture of endothelial cells on gas exchange membranes under inflammatory conditions imitated by the addition of LPS-activated PBMCs. Essential differences have been previously observed in the endothelial cell response to cytokine induction in static versus dynamic culture conditions, indicating the importance of evaluating the endothelial cell response to inflammation under dynamic culture conditions [37].

Optical evaluation of endothelial cell layer after inflammatory treatment showed loss of endothelial cell layer confluence, also confirmed by loss of cell-cell junctions through loss of CD31/PECAM-1 protein expression. Interestingly, CD31/PECAM-1 expression significantly decreased in endothelial cells under inflammatory conditions not only on protein, but also on mRNA level. CD31/PECAM-1 has been previously shown to regulate vascular permeability, as well as inhibit the activation of circulating platelets and leukocytes [38]. Combination of TNFα and IFNγ cytokines has been reported to decrease CD31/PECAM-1 surface expression [39]. Consistent with these findings, we observed upregulation of TNFα gene expression in endothelial cells which could have led to CD31/PECAM-1 inhibition and loss of cell-cell adhesions. Notably, that both endothelial cells and PBMCs could express TNFα [40, 41]. In the used setup, the cells were lyzed for RNA isolation directly from the microfluidic system,

without separation of endothelial cells from potentially attached PBMCs in interest of time to process samples for RNA isolation. Collection of RNA from PBMCs was isolated from the cell-medium-suspension, such that no adherent endothelial cells were included. In order to distinguish between the effects coming from endothelial cells and PBMCs, principal component analysis (PCA) was performed. Here, we showed that the investigated gene expression is different in endothelial cells and PBMCs, with no overlap between the sample clusters. According to the PCA evaluation of qPCR results, the TNFα gene expression primarily occurs in LPS-activated PBMCs, with little to no effect in endothelial cells. Thus, we assume that the reduction in CD31/PECAM-1 expression in endothelial cells due to increased TNFα expression results from the co-culture with LPS-activated PBMCs.

No considerable change has been observed in vWF expression at the protein as well as mRNA level. It has been previously shown that increased vWF expression in septic patients is associated with higher mortality [42] and that inflammation in general can promote increased vWF expression [43, 44]. Since no changes in vWF expression were observed, we investigated gene expression of several genes known to be associated with vWF expression. Specifically, decreased TM and VE-Cadherin expression were reported to be directly affiliated with an increased vWF expression [45-47]. Consistent with the absence of changes in vWF expression, no change in the expression of TM and VE-Cadherin was detected after endothelial cell culture under inflammatory conditions. We assume that the increase in vWF expression would occur in endothelial cells at a later time point than the evaluated 24h.

In the body, leukocyte adhesion is an essential part of the defence mechanisms during inflammation. Under non-inflammatory conditions, leukocytes rapidly move over the endothelial cell layer without adherence. After activation, leukocytes tend to accumulate around the site of inflammation [48]. Leukocytes start a rolling movement along the endothelial cells, attaching to the endothelial cell adhesion molecule E-Selectin [49]. ICAM-1 and VCAM-1, as ligands for lymphocyte function adhesion molecule-1 (LFA-1) and very late activation antigen-4 (VLA-4), respectively, then allow leukocytes to firmly adhere to the endothelial cells [50]. Following, leukocytes transmigrate through the endothelial cell layer towards the inflamed tissue. Although a necessary and reversible process during healthy vascular physiology, leukocyte transmigration might result in vascular leak, expanding permeability of endothelial cell layer in pathological conditions [51]. Consistent with the in-vivo reaction of endothelial cells to inflammation, we observed an increase in endothelial cell adhesion molecules E-Selectin, ICAM-1 and VCAM-1 on a surface protein and gene expression level. These results confirm endothelial cell activation resulting in increased leukocyte adhesion after culture under inflammatory conditions. As there is no tissue below the endothelial cells on a gas exchange membrane in a biohybrid lung, the leukocytes cannot move anywhere after migrating through the endothelial cell layer. We assume that this further promotes the cell detachment and restricts the endothelial cell layer from restricting the leukocyte transmigration and restoring the confluence.

Because cyto- and chemokine expression is an important mechanism for intercellular communication, we evaluated the gene expression of several pro- and anti-inflammatory factors. Upregulation of IL6, IL8, and MCP-1 gene expression in endothelial cells under inflammatory conditions confirms cell activation. It has been previously shown, that increased

IL-6, IL-8 and MCP-1 expression is associated with vascular leakage under septic conditions, which is consistent with our study's results [52]. Additionally, MCP-1 is responsible for attracting leukocytes to the site of injury, which might lead to further endothelial cell layer damage in a biohybrid lung model [53]. In contrast, IL10 acts as an anti-inflammatory cytokine. IL10 has been shown to inhibit pro-inflammatory cytokine production, i.e. TNFα and IFNγ, and support wound healing and tissue repair [54, 55]. In our study, a significant increase in IL10 gene expression was detected under inflammatory conditions. PCA revealed that IL10, similar to TNFα, is mostly expressed by PBMCs and not endothelial cells in the microfluidic system. Thus, we assume that the observed upregulation of IL10 comes as an effect from the RNA being isolated from endothelial cells with the attached PBMCs. Altogether, IL10 expressed by PBMCs might be a potential treatment target to decrease pro-inflammatory cytokine expression and promote endothelial cell layer recovery.

NOS3 is responsible for nitric oxide (NO) production, and thus reduces platelet reactivity and thrombogenicity of endothelial cells [56]. The significant reduction in NOS3 gene expression in endothelial cells under inflammatory conditions would lead to a decrease in NO production. In a biohybrid lung setup, this in turn might lead to an increased thrombosis risk in patients with inflammation. It has been previously shown that NOS3 protects against systemic inflammation while reducing ICAM-1 and IL6 expression, which makes it an interesting potential therapeutic target for inflammation treatment [57]. During inflammation, the disruption of vascular homeostasis leads to upregulation of EDN1, which acts as an antagonist to NOS3 [58]. This behaviour of EDN1 has been confirmed by our investigation of EDN1 gene expression, showing a significant upregulation in endothelial cells under inflammatory conditions. It has been previously shown that LPS-induced sepsis is associated with increased EDN1 expression [59]. In endothelial cells, EDN1 binds to endothelin receptor type B (ETB) that leads to an increased NOS3 activation, and in turn caused NO-induced vasodilation [60]. In general, reduced expression of NOS3 and increased expression of EDN1 in endothelial cells during inflammation points to endothelial cell dysfunction due to KLF2 expression destabilisation [61].

The presented model allowed us to investigate the endothelium for the application in a biohybrid lung model in inflammatory conditions for the first time. We deem this essential before proceeding with (pre-) clinical studies to proof the concept of biohybrid lungs. Here, we would like to emphasize the importance of biohybrid device testing in conditions similar to later application in patients. A condition such as inflammation can drastically influence the potential results as shown in this study. Yet, having a model system to detect challenges and pitfalls during device development allows setup adaptation before failure in preclinical or even clinical testing under relevant conditions. The observed loss of endothelial cell layer integrity on a gas exchange membrane puts a big question mark on the concept of oxygenator endothelialization proposed and investigated by us and others. An endothelial layer failing already after 24 h under inflammatory conditions would result in blood contact with the artificial surface of the gas exchange membrane thus eliminating all potential advantages of the endothelialization while causing even more severe effects such as thrombus formation by the detaching cell layer. Thus, the presented observations should result in consideration of patient statuses in device design and testing in future studies. We see the described

microfluidic dynamic system as an opportunity to investigate the potential of membrane modifications or new therapeutic targets to eliminate the effects of inflammation on endothelial cells.

Our gas exchange membrane microfluidic model allowed us to successfully investigate endothelial cell behaviour under inflammatory conditions. We are confident that our model can be adapted as a model for septic conditions not only to model biohybrid lung application, but also as a disease model for endothelial behavior in chronic lung and cardiovascular diseases. Here, we presented a model that is easily adaptable to necessary testing conditions: the culture substrate can be exchanged, WSS can be varied, as well as immune blood cell and LPS concentration. Here, we utilized PBMCs activated with LPS as a sepsis model. It is also possible to perform testing with other cell types, such as granulocytes or thrombocytes.

5. Conclusion

In summary, our study shows that endothelial cells do not withstand dynamic culture under inflammatory conditions. Inflammation causes loss of endothelial cell layer confluence, as well as increased leukocyte adhesion. Several inflammation-associated genes are upregulated in endothelial cells after culture with LPS-activated PBMCs to mimic inflammatory conditions. Thus, we conclude that further improvements of endothelialized ECMO devices are necessary to ensure its usability in realistic inflammatory conditions.

Supplementary Material

The following supplementary material is available:

Table S1: Percentage of positive HUVECs (n=4) stained for four endothelial cell-characteristic markers (CD31, CD105, CD144, and CD146) and one mesenchymal stromal cell-characteristic marker.

Table S2: Mean fluorescence intensity (MFI) of ICAM-1, E-Selectin, and VCAM-1 expression measured by flow cytometry of endothelial cells (n=3) under following conditions: no treatment, treatment with LPS, treatment with PBMCs, and treatment with LPS-activated PBMCs.

Table S3. Used primers for qPCR and their annealing temperatures.

Figure S1: Representative images of leukocyte adhesion assay. PBMCs (green) dynamically cultivated on endothelial cells (brightfield) with or without LPS-activation. Scale bar: 100 µm.

Data Availability Statement

The raw data presented in this study are available on request from the corresponding author.

Conceptualization

A.L.T., C.G.C., K.T. and S.J; Formal analysis: M.C. and A.B.; Funding acquisition: K.T., C.G.C., A.L.T. and S.J.; Investigation: M.C., S.K., A.P., S.R. and A.B.; Project administration: C.G.C., A.L.T. , K.T. and S.J.; Resources: S.J.; Supervision: K.O., K.T., A.L., C.G.C., A.L.T., S.J.; Validation: M.C.,

A.B., A.L.T. and S.J., Visualization: M.C. and A.B., Writing – original draft: M.C.; Writing – review & editing: M.C., A.B., C.T.N., S.K., A.P., K.O., K.T., S.R., A.L., C.G.C., A.L.T. and S.J.

Funding

This research was funded by the Deutsche Forschungsgemeinschaft (DFG) in the framework of the priority program "Towards an Implantable Lung" (grant numbers 313779459, 447717028, 447712946 and Start-Funding for Young Female Researcher) and within the Research Training Group 2415 (Project number: 363055819). The Quattro S was funded by the DFG grant number 495328185.

Conflict of Interest Disclosure

The authors declare no conflict of interest. The funders had no role in the design of the study; in the collection, analyses or interpretation of data; in the writing of the manuscript; or in the decision to publish the results.

Ethics Approval Statement

The study was conducted in accordance with the Declaration of Helsinki, and approved by the Ethics Committee of the Medical Faculty of RWTH Aachen University (protocol codes EK 067/18 and EK 22-390).

Patient Consent Statement

Written informed consent was obtained from all subjects involved in the study.

Acknowledgements

The authors would like to thank the Clinic for Gynaecology and Obstetrics RWTH Aachen University Hospital headed by Univ.-Prof. Dr. med. Elmar Stickeler for providing umbilical cord tissue for HUVECs isolation. This work was supported by the Confocal Microscopy Facility headed by Prof. Dr. rer. nat. Gerhard Mueller-Newen, as well as a by the Flow Cytometry Facility headed by Univ.-Prof. Dr. rer. nat. Oliver Pabst, core facilities of the Interdisciplinary Center for Clinical Research (IZKF) Aachen within the Faculty of Medicine at RWTH Aachen University. Figure 1, as well as the graphical abstract were created with Biorender.com.

References

1. Brodie D, Slutsky AS, Combes A. Extracorporeal Life Support for Adults With Respiratory Failure and Related Indications: A Review. JAMA. 2019;322(6):557-68.
2. Paolone S. Extracorporeal Membrane Oxygenation (ECMO) for Lung Injury in Severe Acute Respiratory Distress Syndrome (ARDS): Review of the Literature. Clin Nurs Res. 2017;26(6):747-62.
3. Al-Fares A, Pettenuzzo T, Del Sorbo L. Extracorporeal life support and systemic inflammation. Intensive care medicine experimental. 2019;7(1):1-14.
4. Datzmann T, Traeger K. Extracorporeal membrane oxygenation and cytokine adsorption. Journal of thoracic disease. 2018;10(Suppl 5):S653.
5. Kumar G, Maskey A. Anticoagulation in ECMO patients: an overview. Indian Journal of Thoracic and Cardiovascular Surgery. 2021:1-7.

6. Pflaum M, Peredo AS, Dipresa D, De A, Korossis S. Membrane bioreactors for (bio-)artificial lung. Current Trends and Future Developments on (Bio-) Membranes2020. p. 45-75.
7. Klein S, Hesselmann F, Djeljadini S, Berger T, Thiebes AL, Schmitz-Rode T, Jockenhoevel S, Cornelissen CG. EndOxy: Dynamic Long-Term Evaluation of Endothelialized Gas Exchange Membranes for a Biohybrid Lung. Ann Biomed Eng. 2020;48(2):747-56.
8. Dietrich M, Finocchiaro N, Olszweski S, Arens J, Schmitz-Rode T, Sachweh J, Jockenhoevel S, Cornelissen CG. ENDOXY - Development of a Biomimetic Oxygenator-Test-Device. PLoS One. 2015;10(12):e0142961.
9. Salehi-Nik N, Banikarimi SP, Amoabediny G, Pouran B, Shokrgozar MA, Zandieh-Doulabi B, Klein-Nulend J. Flow preconditioning of endothelial cells on collagen-immobilized silicone fibers enhances cell retention and antithrombotic function. Artificial organs. 2017;41(6):556-67.
10. Polk AA, Maul TM, McKeel DT, Snyder TA, Lehocky CA, Pitt B, Stolz DB, Federspiel WJ, Wagner WR. A biohybrid artificial lung prototype with active mixing of endothelialized microporous hollow fibers. Biotechnology and bioengineering. 2010;106(3):490-500.
11. Alabdullh HA, Pflaum M, Mälzer M, Kipp M, Naghilouy-Hidaji H, Adam D, Kühn C, Natanov R, Niehaus A, Haverich A, Wiegmann B. Biohybrid Lung Development: Towards Complete Endothelialization of an Assembled Extracorporeal Membrane Oxygenator. Bioengineering. 2023;10(1).
12. Wiegmann B, von Seggern H, Hoffler K, Korossis S, Dipresa D, Pflaum M, Schmeckebier S, Seume J, Haverich A. Developing a biohybrid lung - sufficient endothelialization of poly-4-methly-1-pentene gas exchange hollow-fiber membranes. J Mech Behav Biomed Mater. 2016;60:301-11.
13. Zimmerman JL. Respiratory failure. Blood purification. 2002;20(3):235-8.
14. Kaku S, Nguyen CD, Htet NN, Tutera D, Barr J, Paintal HS, Kuschner WG. Acute respiratory distress syndrome: etiology, pathogenesis, and summary on management. Journal of Intensive Care Medicine. 2020;35(8):723-37.
15. Baniya S, Shrestha TM, Pant P, Aacharya RP. Metabolic Syndrome among Stable Chronic Obstructive Pulmonary Disease Patients Visiting Outpatient Department of a Tertiary care centre: A Descriptive Cross-sectional Study. JNMA: Journal of the Nepal Medical Association. 2023;61(260):355.
16. Wang Y, Cao P. Extracorporeal membrane oxygenation (ECMO) for acute exacerbations of chronic obstructive pulmonary disease: care modalities, experience, and precautions. American Journal of Translational Research. 2021;13(5):4922.
17. Thangappan K, Cavarocchi NC, Baram M, Thoma B, Hirose H. Systemic inflammatory response syndrome (SIRS) after extracorporeal membrane oxygenation (ECMO): Incidence, risks and survivals. Heart & Lung. 2016;45(5):449-53.
18. Millar JE, Fanning JP, McDonald CI, McAuley DF, Fraser JF. The inflammatory response to extracorporeal membrane oxygenation (ECMO): a review of the pathophysiology. Critical care. 2016;20(1):1-10.
19. Ince C, Mayeux PR, Nguyen T, Gomez H, Kellum JA, Ospina-Tascón GA, Hernandez G, Murray P, De Backer D, Workgroup obotAX. The Endothelium in Sepsis. Shock. 2016;45(3):259-70.
20. Hennigs JK, Matuszcak C, Trepel M, Körbelin J. Vascular endothelial cells: heterogeneity and targeting approaches. Cells. 2021;10(10):2712.
21. Joffre J, Hellman J, Ince C, Ait-Oufella H. Endothelial responses in sepsis. American journal of respiratory and critical care medicine. 2020;202(3):361-70.
22. Sutton NR, Baek A, Pinsky DJ. Endothelial Cells and Inflammation. In: Mackay IR, Rose NR, Diamond B, Davidson A, editors. Encyclopedia of Medical Immunology: Autoimmune Diseases. New York, NY: Springer New York; 2014. p. 367-81.
23. Szmitko PE, Wang C-H, Weisel RD, Almeida JRd, Anderson TJ, Verma S. New Markers of Inflammation and Endothelial Cell Activation. Circulation. 2003;108(16):1917-23.
24. Theofilis P, Sagris M, Oikonomou E, Antonopoulos AS, Siasos G, Tsioufis C, Tousoulis D. Inflammatory mechanisms contributing to endothelial dysfunction. Biomedicines. 2021;9(7):781.

25. Hellenthal KE, Brabenec L, Wagner N-M. Regulation and dysregulation of endothelial permeability during systemic inflammation. Cells. 2022;11(12):1935.
26. Wettschureck N, Strilic B, Offermanns S. Passing the vascular barrier: endothelial signaling processes controlling extravasation. Physiological reviews. 2019;99(3):1467-525.
27. Menzel S, Finocchiaro N, Donay C, Thiebes AL, Hesselmann F, Arens J, Djeljadini S, Wessling M, Schmitz-Rode T, Jockenhoevel S, Cornelissen CG. Towards a Biohybrid Lung: Endothelial Cells Promote Oxygen Transfer through Gas Permeable Membranes. Biomed Res Int. 2017;2017:5258196.
28. Li B, Chen J, Wang JH. RGD peptide-conjugated poly(dimethylsiloxane) promotes adhesion, proliferation, and collagen secretion of human fibroblasts. J Biomed Mater Res A. 2006;79(4):989-98.
29. Stirling DR, Swain-Bowden MJ, Lucas AM, Carpenter AE, Cimini BA, Goodman A. CellProfiler 4: improvements in speed, utility and usability. BMC bioinformatics. 2021;22:1-11.
30. Cheremkhina M, Klein S, Babendreyer A, Ludwig A, Schmitz-Rode T, Jockenhoevel S, Cornelissen CG, Thiebes AL. Influence of Aerosolization on Endothelial Cells for Efficient Cell Deposition in Biohybrid and Regenerative Applications. Micromachines. 2023;14(3):575.
31. Ruijter J, Ramakers C, Hoogaars W, Karlen Y, Bakker O, Van den Hoff M, Moorman A. Amplification efficiency: linking baseline and bias in the analysis of quantitative PCR data. Nucleic acids research. 2009;37(6):e45-e.
32. Pedregosa F, Varoquaux G, Gramfort A, Michel V, Thirion B, Grisel O, Blondel M, Prettenhofer P, Weiss R, Dubourg V. Scikit-learn: Machine learning in Python. the Journal of machine Learning research. 2011;12:2825-30.
33. Pflaum M, Jurmann S, Katsirntaki K, Malzer M, Haverich A, Wiegmann B. Towards Biohybrid Lung Development-Fibronectin-Coating Bestows Hemocompatibility of Gas Exchange Hollow Fiber Membranes by Improving Flow-Resistant Endothelialization. Membranes (Basel). 2021;12(1).
34. Zwirner U, Hoffler K, Pflaum M, Korossis S, Haverich A, Wiegmann B. Identifying an optimal seeding protocol and endothelial cell substrate for biohybrid lung development. J Tissue Eng Regen Med. 2018;12(12):2319-30.
35. Siedlecki C. Hemocompatibility of biomaterials for clinical applications: Blood-biomaterials interactions: Woodhead Publishing; 2018.
36. Wu J, Deng Z, Sun M, Zhang W, Yang Y, Zeng Z, Wu J, Zhang Q, Liu Y, Chen Z. Polydatin protects against lipopolysaccharide-induced endothelial barrier disruption via SIRT3 activation. Laboratory Investigation. 2020;100(4):643-56.
37. Shaw SK, Perkins BN, Lim Y-C, Liu Y, Nusrat A, Schnell FJ, Parkos CA, Luscinskas FW. Reduced expression of junctional adhesion molecule and platelet/endothelial cell adhesion molecule-1 (CD31) at human vascular endothelial junctions by cytokines tumor necrosis factor-α plus interferon-γ does not reduce leukocyte transmigration under flow. The American journal of pathology. 2001;159(6):2281-91.
38. Lertkiatmongkol P, Liao D, Mei H, Hu Y, Newman PJ. Endothelial functions of PECAM-1 (CD31). Current opinion in hematology. 2016;23(3):253.
39. Woodfin A, Voisin M-B, Nourshargh S. PECAM-1: a multi-functional molecule in inflammation and vascular biology. Arteriosclerosis, thrombosis, and vascular biology. 2007;27(12):2514-23.
40. Lee DK, Nevo O. Tumor necrosis factor alpha expression is increased in maternal microvascular endothelial cells in preeclampsia. Hypertension in Pregnancy. 2021;40(3):193-201.
41. Alinejad S, Khademvatan S, Amani S, Asadi N, Tappeh KH, Yousefi E, Miandoabi T. The Effect of Curcumin on the Expression of INFγ, TNF-α, and iNOS Genes in PBMCs Infected with Leishmania major [MRHO/IR/75/ER]. Infectious Disorders-Drug Targets (Formerly Current Drug Targets-Infectious Disorders). 2022;22(6):83-9.
42. Ware LB, Eisner MD, Thompson BT, Parsons PE, Matthay MA. Significance of von Willebrand factor in septic and nonseptic patients with acute lung injury. American journal of respiratory and critical care medicine. 2004;170(7):766-72.
43. Sumpio BE, Riley JT, Dardik A. Cells in focus: endothelial cell. The international journal of biochemistry & cell biology. 2002;34(12):1508-12.

44. Chen J, Chung DW. Inflammation, von Willebrand factor, and ADAMTS13. Blood, The Journal of the American Society of Hematology. 2018;132(2):141-7.
45. Giri H, Panicker SR, Cai X, Biswas I, Weiler H, Rezaie AR. Thrombomodulin is essential for maintaining quiescence in vascular endothelial cells. Proceedings of the National Academy of Sciences. 2021;118(11):e2022248118.
46. Won T, Wood MK, Hughes DM, Talor MV, Ma Z, Schneider J, Skinner JT, Asady B, Goerlich E, Halushka MK. Endothelial thrombomodulin downregulation caused by hypoxia contributes to severe infiltration and coagulopathy in COVID-19 patient lungs. EBioMedicine. 2022;75.
47. Morini MF, Giampietro C, Corada M, Pisati F, Lavarone E, Cunha SI, Conze LL, O'Reilly N, Joshi D, Kjaer S. VE-Cadherin–Mediated epigenetic regulation of endothelial gene expression. Circulation research. 2018;122(2):231-45.
48. van de Vijver E, van den Berg TK, Kuijpers TW. Leukocyte adhesion deficiencies. Hematology/Oncology Clinics. 2013;27(1):101-16.
49. Rosen SD, Bertozzi CR. Leukocyte adhesion: two selectins converge on sulphate. Current Biology. 1996;6(3):261-4.
50. Lawson C, Wolf S. ICAM-1 signaling in endothelial cells. Pharmacological reports. 2009;61(1):22-32.
51. Weis SM. Evaluating vascular leak in vivo. Methods in enzymology. 2008;444:99-114.
52. Kang S, Kishimoto T. Interplay between interleukin-6 signaling and the vascular endothelium in cytokine storms. Experimental & molecular medicine. 2021;53(7):1116-23.
53. Singh S, Anshita D, Ravichandiran V. MCP-1: Function, regulation, and involvement in disease. International immunopharmacology. 2021;101:107598.
54. Moore KW, de Waal Malefyt R, Coffman RL, O'Garra A. Interleukin-10 and the interleukin-10 receptor. Annual review of immunology. 2001;19(1):683-765.
55. Short WD, Steen E, Kaul A, Wang X, Olutoye OO, Vangapandu HV, Templeman N, Blum AJ, Moles CM, Narmoneva DA. IL-10 promotes endothelial progenitor cell infiltration and wound healing via STAT3. The FASEB Journal. 2022;36(7).
56. Oliveira-Paula GH, Lacchini R, Tanus-Santos JE. Endothelial nitric oxide synthase: From biochemistry and gene structure to clinical implications of NOS3 polymorphisms. Gene. 2016;575(2):584-99.
57. Bougaki M, Searles RJ, Kida K, De Yu J, Buys ES, Ichinose F. Nos3 protects against systemic inflammation and myocardial dysfunction in murine polymicrobial sepsis. Shock (Augusta, Ga). 2010;34(3):281.
58. Gupta A. An Overview of Gene Variants of Endothelin-1: A Critical Regulator of Endothelial Dysfunction. Endothelial Dysfunction-A Novel Paradigm. 2022.
59. Kowalczyk A, Kleniewska P, Kolodziejczyk M, Skibska B, Goraca A. The role of endothelin-1 and endothelin receptor antagonists in inflammatory response and sepsis. Archivum immunologiae et therapiae experimentalis. 2015;63:41-52.
60. Enevoldsen FC, Sahana J, Wehland M, Grimm D, Infanger M, Krüger M. Endothelin receptor antagonists: status quo and future perspectives for targeted therapy. Journal of Clinical Medicine. 2020;9(3):824.
61. Dabravolski SA, Sukhorukov VN, Kalmykov VA, Grechko AV, Shakhpazyan NK, Orekhov AN. The role of KLF2 in the regulation of atherosclerosis development and potential use of KLF2-targeted therapy. Biomedicines. 2022;10(2):254.